Optical Review (2024) 31:135–143
https://doi.org/10.1007/s10043-023-00854-4

SPECIAL SECTION: REGULAR PAPER

Laser Display and Lighting Conference (LDC' 23), Yokohama, Japan

Increasing vection strength by video processing in the periphery of the visual field in a driving simulator

Kosuke Nakanishi[1] · **Haruki Mizushina**[1] · **Kenji Yamamoto**[1]

Received: 20 June 2023 / Accepted: 17 November 2023 / Published online: 21 December 2023

Abstract

In this paper, we propose a method to increase vection strength through video image processing in the periphery, rather than the center, of the visual field. Specifically, we propose two methods. One is an image stretching process in the visual periphery and the other is an alpha-blending process with an expanding circle grating in the periphery of the field. We clarified the relationship between the processing conditions and vection strength and found that stretching in the left–right direction increased vection strength while stretching in the downward direction did not. When adding expanding grating by alpha-blending, vection strength and duration were increased in almost all cases.

Keywords Vection · Video processing · Alpha blending · Stretching process · Periphery of the visual field

1 Introduction

The perception generated by a driving simulation is quite different from actual driving. Reasons for the difference are the lack of self-motion and immersion. Such shortcomings in a four-wheeled vehicle driving simulation limit the effectiveness of the training. Furthermore, these deficiencies are more serious in the case of a motorcycle driving simulation because the driver must pay attention to his/her body posture, maintain balance, and move his/her body quickly according to the sense of self-motion. Therefore, the lack of self-motion perception is a very serious issue in driving simulations, especially in motorcycle driving simulations.

In a driving simulation, increasing vection strength is a promising way to increase the sense of self-motion. Vection is a phenomenon that makes the person feel that they are moving through visual information only, even if he/she does not actually move. Because the drivers perceive the environment mainly from visual information [1], we expect this approach to work well for driving simulations.

To induce stronger vection, we propose two methods. These methods enhance vection by increasing the optical flow in the periphery of the visual field. Previous studies [2–4] induced vection by the same means. However, our method increases the optical flow in the periphery of the field of view and at the same time allows the observer to see what is going on around them.

The first method, named the "stretching process," stretches the video image outward in the periphery of the visual field. To the best of the authors' knowledge, there have been no previous studies that have stretched the image in the periphery of the visual field to increase vection strength. The fact that the optical flow is increased using the original image without synthesizing new visual stimuli is also unique as a method for enhancing vection.

The second method, "adding expanding circle grating," is the process of superimposing white-black stripes in the periphery of the visual field and moving the stripes outward quickly. Suzuki et al. conducted almost the same method [5], but their study differs from our experiment in three ways. First, their purpose was to indicate the traveling direction to a traveler on a personal mover. Second, their experiment used visual stimuli that elicited lateral vection, whereas our

✉ Kosuke Nakanishi
c612336002@tokushima-u.ac.jp

Haruki Mizushina
mizushina.haruki@tokushima-u.ac.jp

Kenji Yamamoto
kenji.yamamoto@tokushima-u.ac.jp

[1] Department of Optical Science and Technology, Tokushima University, 2-1 Minami-Jyosanjima-cho, Tokushima 770-8506, Japan

experiment uses visual stimuli that enhance forward vection. Third, Suzuki et al.'s experiment used stimuli that did not penetrate the background; in our experiment, in contrast, we added stimuli in the periphery of the visual field to the extent that the background penetrated the visual field and could be seen. Thus, our method is novel in that it allows us to confirm the surrounding situation.

We apply the "stretching process" and "adding expanding circle grating" only in the periphery of the visual field in this study because we fear the risk that image processing in the center will disturb the driver's concentration; there is the risk that the driver will waste considerable time identifying road signs and traffic lights if the image in the gazing viewing area is processed unnaturally. This wasted time worsens the effect of the driving training. In addition, Konishi et al. have successfully induced stronger vection by their original image processing in the periphery of the visual field [6], which suggests the potential of the periphery of the visual field to increase vection strength. If strong vection occurs by only image processing in the periphery of the visual field without any expensive equipment [7], this technology contributes to a new and effective driving simulator and can be applied to other simulators.

In this paper, we propose and define our two methods in Sect. 2. We explain the methods and the results of our evaluation experiments on vection strength to confirm the effectiveness of the two proposed methods in Sects. 3 and 4. Finally, we present our conclusions in Sect. 5.

2 Proposed video processing

2.1 Stretching process

In this study, we presented 180°-surrounding video images to the subjects using a head mounted display (HMD). We explain the details of the image processing method, including coordinate transformation, in this section.

Assume that the images before and after stretching are denoted by $Image_{in}(h_A, w_A)$ and $Image_{out}(h_A, w_A)$, and each pixel position is expressed by $Q(h_{in}, w_{in})$ and $P(h_{out}, w_{out})$ as points on the images, as shown in Fig. 1. h_A and w_A are the number of pixels in $Image_{in}$ and $Image_{out}$, respectively, and the image size does not change before and after the stretching process. The head of the image observer is located at the center of the sphere in Fig. 2(a) and the head observes the image with the positive direction of the x-axis in front. At this time, $Image_{out}$ is stuck to the surface of the hemisphere of radius 1 with the center at point O, as shown in Fig. 2(b). The stretching process first transforms point $P(h_{out}, w_{out})$ into a spherical coordinate $P(1, \theta_{out}, \varphi_{out})$. This transformation is expressed as follows, when the angle formed by the z-axis and OP is θ_{out}

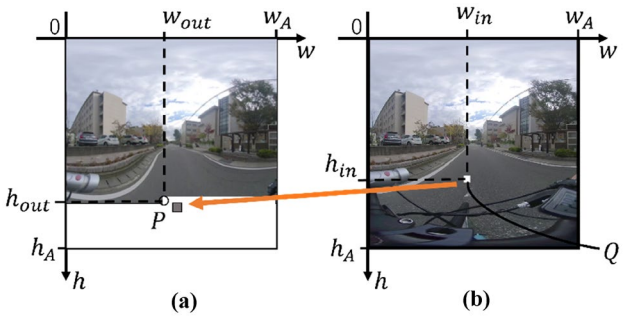

Fig. 1 Coordinate settings before and after stretching process. **a** Image after processing; **b** original image

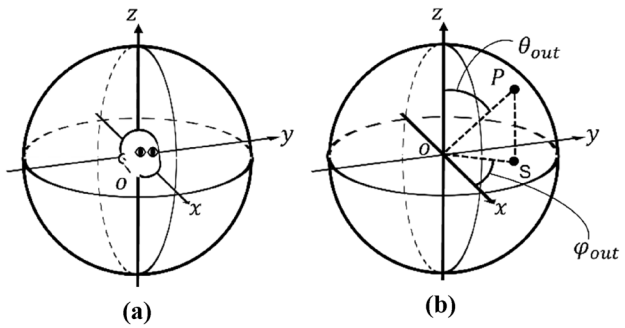

Fig. 2 Setting image coordinates

[rad] and the angle formed by the x-axis and point S, which is perpendicular to the xy-plane from point P, is φ_{out} [rad]:

$$\theta_{\text{out}} = \frac{\pi h_{\text{out}}}{h_A}, \tag{1}$$

$$\varphi_{\text{out}} = \frac{\pi w_{\text{out}}}{w_A} - \frac{\pi}{2}. \tag{2}$$

Next, the process moves point P along the θ-axis or φ-axis. Let point $Q(1, \theta_{in}, \varphi_{in})$ be the point after moving point $P(1, \theta_{out}, \varphi_{out})$ by ω [rad] on the φ axis. This step is defined as follows:

$$\theta_{\text{in}} = \theta_{\text{out}}, \tag{3}$$

$$\varphi_{\text{in}} = \varphi_{\text{out}} - \omega. \tag{4}$$

ω is defined as

$$\omega = (\varphi_{\text{out}} + R)(1 - k)(\varphi_{\text{out}} < -R), \tag{5}$$

$$\omega = 0(-R \le \varphi_{\text{out}} \le R), \tag{6}$$

$$\omega = \left(\varphi_{\text{out}} - R\right)(1-k)\left(R < \varphi_{\text{out}}\right), \tag{7}$$

where R and k are the un-processing range and a value representing the degree of stretching (hereafter these are referred to as the un-processing range parameter and stretching magnification), respectively.

Next, the process transforms spherical coordinates $P\left(1, \theta_{out}, \varphi_{out}\right)$ into Cartesian linear coordinates $P\left(x_{out}, y_{out}, z_{out}\right)$, whose coordinates are expressed as

$$x_{\text{out}} = \sin\theta_{\text{out}} \cos\varphi_{\text{out}}, \tag{8}$$

$$y_{\text{out}} = \sin\theta_{\text{out}} \sin\varphi_{\text{out}}, \tag{9}$$

$$z_{\text{out}} = \cos\theta_{\text{out}}. \tag{10}$$

Next, it rotates $P\left(x_{out}, y_{out}, z_{out}\right)$ to $Q\left(x_{in}, y_{in}, z_{in}\right)$ by angle ω around the φ- axis.

$$x_{\text{in}} = x_{\text{out}} \cos(-\omega) + z_{\text{out}} \sin(-\omega), \tag{11}$$

$$y_{\text{in}} = -x_{\text{out}} \sin(-\omega) + z_{\text{out}} \cos(-\omega), \tag{12}$$

$$z_{\text{in}} = z_{\text{out}}. \tag{13}$$

Next, the Cartesian linear coordinates $Q\left(x_{in}, y_{in}, z_{in}\right)$ are transformed to the spherical coordinates $Q(r_{in}, \theta_{in}, \varphi_{in})$.

$$r_{\text{in}} = \sqrt{x_{\text{in}}^2 + y_{\text{in}}^2 + z_{\text{in}}^2}, \tag{14}$$

$$\theta_{\text{in}} = \cos^{-1} \frac{z_{\text{in}}}{\sqrt{x_{\text{in}}^2 + y_{\text{in}}^2 + z_{\text{in}}^2}}, \tag{15}$$

$$\varphi_{\text{in}} = sgn\left(y_{\text{in}}\right) \cos^{-1} \frac{x_{in}}{\sqrt{x_{\text{in}}^2 + y_{\text{in}}^2 + z_{\text{in}}^2}}. \tag{16}$$

Finally, point Q is transformed from $\left(1, \theta_{in}, \varphi_{in}\right)$ to (h_{in}, w_{in}) using the following formula to create $Image_{out}$.

$$h_{\text{in}} = h_A \frac{\theta_{\text{in}}}{\pi}, \tag{17}$$

$$w_{\text{in}} = w_A \left(\frac{\varphi_{\text{in}}}{\pi} + 0.5\right). \tag{18}$$

The above defines only for φ-axis movement, but θ-axis movement can be defined in the same way.

2.2 Adding expanding grating

The adding expanding grating process adds a black-and-white stripe pattern that moves continuously from the center toward the periphery (hereafter referred to as expanding grating) into the live-action video. The expanding grating is created with computer graphics by moving the camera forward at a constant linear velocity of s km/h through a tunnel covered with a series of black-and-white striped textures and a diameter of d m. This process can be done simply using OmegaSpace software [8]. Figure 3 shows an example of the expanding grating that is used to generate trial videos.

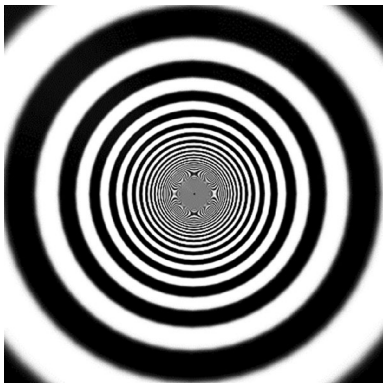

Fig. 3 Example of expanding grating

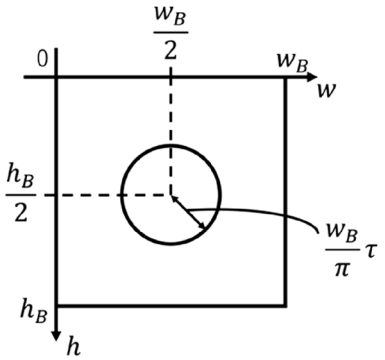

Fig. 4 Circle coordinate setting

For adding, we used the alpha blending shown in Eq. (19).

$$(1-\alpha)\boldsymbol{c}_1 + \alpha\boldsymbol{c}_2 = \boldsymbol{c}_3, \tag{19}$$

where $\boldsymbol{c}_1$,$\boldsymbol{c}_2$, and $\boldsymbol{c}_3$ are the live-action image, black-and-white stripe pattern image, and trial image, respectively, and α is the constant value (hereafter referred to as the adding coefficient).

Assume that the number of vertical and horizontal pixels of the live-action video is set to h_B and w_B, respectively. As shown in Fig. 4, a circle C expressed by the following equation can be drawn in the center of the image with the origin at the upper left corner of the image.

$$\left(w-\frac{w_B}{2}\right)^2+\left(h-\frac{h_B}{2}\right)^2=\left(\frac{w_B}{\pi}\tau\right)^2. \quad (20)$$

This process applies Eq. (20) only outside of the circle C that is defined by τ [rad] (hereafter referred to as the un-processing range parameter) so as not to disturb the driver.

3 Experimental procedure

3.1 Experimental setup

For capturing live-action video, we used the Insta360 EVO camera [9], which can capture 180°-surrounding stereo video with a resolution of 3840 × 1920 pixels and a frame rate of 50 fps. The distance between stereo lenses is 65 mm. We moved this camera straight ahead at a speed of approximately 30 km/h during the 10-s shooting of the live-action video.

For displaying the 180°-surrounding stereo video, we used a VIVE Pro [10] HMD (Head Mounted Display) and VIVEPORT Video software [11] with an all-surrounding view setting of 1440 × 1600 pixels per eye (2880 × 1600 pixels for both eyes) and a refresh rate of 90 Hz. A mouse was used to measure the duration and latency of the vection.

In Experiments 1 and 2, we tried to clarify whether vection was induced by the stretching process or adding expanding grating to the live-action video in which the conditions and vection strength were increased.

The subjects were seated wearing the HMD and instructed to observe the center of the image and press the mouse button while they perceived vection during a one-condition video. The latency is defined as the time from the start of the one-condition video to the first press of the mouse button. The duration is defined as the total time during which the mouse button was pressed. We included a one-minute break between each trial in the video set. This one-minute break was provided to minimize the influence of vection between trial videos. During the breaks between the videos, the subjects were asked to subjectively rate the perceived vection strength on a scale of 0 (no vection) to 100 (very strong vection), as was done in similar previous studies [12–15] that measured vection strength.

Eight male subjects (22–24 years of age) participated. All subjects were in good health and had normal or corrected-to-normal vision.

3.2 Stretching process and video sets

The images were stretched in the left–right or downward direction.

For left–right stretching, we set un-processing range parameter $R=\frac{\pi}{18}$ or $\frac{\pi}{9}$; that is, the un-processing range is $-\frac{\pi}{18}\le\varphi_{out}\le\frac{\pi}{18}$ or $-\frac{\pi}{9}\le\varphi_{out}\le\frac{\pi}{9}$.

For downward stretching, we set $R=\frac{\pi}{18}$ or $\frac{\pi}{9}$; that is, the un-processing range is $0\le\theta_{out}\le\frac{\pi}{18}+\frac{\pi}{2}$ or $0\le\theta_{out}\le\frac{\pi}{9}+\frac{\pi}{2}$. Because the processing is only downward and the origin of θ_{out} is the ceiling, the beginning is zero and the ending is added $\frac{\pi}{2}$, respectively.

We also set stretching magnification factor $k=1.00, 1.25, 1.33, 1.43$ and 1.67 (1.00 is equivalent to no image processing). Figure 5 shows an example of a processed image of downward stretching with $k=1.67$, $R=\frac{\pi}{18}$.

We first created two types of video sets: one for the left–right direction and the other for the downward direction. Each video set included one no-processing video and eight processed videos with combinations of the four conditions of the stretching magnification and the two un-processing range parameters R. Each video set consisted of these nine trial videos in random order with one-minute breaks between trials. We displayed the video sets three times each for the downward and left–right directions.

3.3 Expanding grating and video sets

We used the same live-action video as in Experiment 1.

In the generation of the expanding grating videos, we set camera movement speed $s=30$ and tunnel diameter coefficient $d=4$ to film the video.

In this processing, four conditions were set for the adding coefficient, $\alpha=0.00$ (no processing), 0.05, 0.1, and 0.2, and

Fig. 5 Example of trial video (with downward stretching process and k = 1.67, R = π/18)

three conditions were set for the radius of the viewing angle of the un-processing range, $\tau = \frac{\pi}{18}, \frac{\pi}{12}$, and $\frac{\pi}{9}$.

We first created a total of 10 trial videos including one no-processing video and nine trial videos with combinations of the un-processing range and adding coefficient conditions. An example is shown in Fig. 6.

Next, we created three video sets including those ten trial videos in random order with one-minute breaks between trials. The subjects observed three video sets.

4 Results and discussion

4.1 Experiment 1: evaluation of stretching process for increasing vection strength

Figures 7(a, b) and 8(a, b) show the results of vection strength, latency, and duration for the un-processing range of $R = \frac{\pi}{18}$ in the left–right direction, $R = \frac{\pi}{9}$ in the left–right direction, $R = \frac{\pi}{18}$ in the downward direction, and $R = \frac{\pi}{9}$ in the downward direction, respectively. In each graph, the horizontal axis indicates image magnification factor k and the vertical axis indicates the evaluated value. Data from different subjects are plotted with different symbols. Each plot shows an average of three trials.

In the left–right direction, as shown in Fig. 7, the vection strength tends to increase for the stretched video compared to the no-processing video, and vection increases stably and strongly at $k = 1.43$ and $R = \frac{\pi}{18}$ except for Subject 3. As shown in Fig. 7 (a), the vection strength on $R = \frac{\pi}{18}$ increases up to $k = 1.43$ followed by a decreasing trend of k down to $k = 1.67$. Figure 7 shows no consistent trend in latency and duration among the subjects. According to the subjects' introspection reports, unnaturalness increases in the processed range when the stretching magnification is increased. Therefore, even if the speed of optical flow in the periphery of the visual field increased, the vection strength decreased due to the unnaturalness in the processed range.

In Figs. 7 and 8, the vection strength of Subject 3 decreases when the stretching magnification increases both in the left–right and downward directions. This may be because this subject perceived sufficiently strong vection even in the unprocessed (k = 0) video, and the unnaturalness caused by the stretching process may have impaired the vection strength.

In the downward direction, Fig. 8(a) shows that the vection strength of Subjects 3 and 6 decreases as the magnification increases at $R = \frac{\pi}{18}$, but there is no significant difference between magnification factor $k = 1.00$ and other magnifications for most of the subjects, suggesting that the downward direction stretching process does not increase vection strength. The graphs in Fig. 8 show no consistent trend in latency or duration among subjects.

In the downward direction, the vection strength is almost the same regardless of the magnification factor. This is because the ground surface was asphalt, which creates little optical flow and is less effective for inducing vection, so the visual stimuli do not increase even after the stretching process is applied. Therefore, the effectiveness of the downward stretching may be clarified by conducting experiments using video that includes rich optical flow that induces stronger visual stimuli.

4.2 Experiment 2: evaluation of adding expanding grating for increasing vection strength

Figure 9(a), (b), and (c) shows the results of vection strength, latency, and duration when subjects viewed an adding image of a live-action video with expanding grating at $\tau = \frac{\pi}{18}, \frac{\pi}{12}$, and $\frac{\pi}{9}$, respectively. The horizontal and vertical axes indicate adding coefficient and evaluated value, respectively. These evaluated values are averaged over three trials for each subject.

Figure 9(a), (b), and (c) shows that vection strength and duration increases or becomes nearly flat when adding coefficient $\alpha = 0.05$ and 0.1 as compared to $\alpha = 0$ for all un-processing range τ. This indicates that adding processing increases vection strength. At $\alpha = 0.05$, vection strength increased or became nearly flat for all subjects compared to when $\alpha = 0$. For Subjects 5 and 8, duration is stable at 8 to 10 s for all adding coefficients. As shown in Fig. 9(a), (b), and (c), the vection strength of each subject was the highest around $\alpha = 0.05$ or $\alpha = 0.1$ for all adding coefficients. For example, at $\tau = \frac{\pi}{9}$ in Fig. 9(a), Subject 5 showed the highest

Fig. 6 Example of trial video (α = 0.2, τ = 20°)

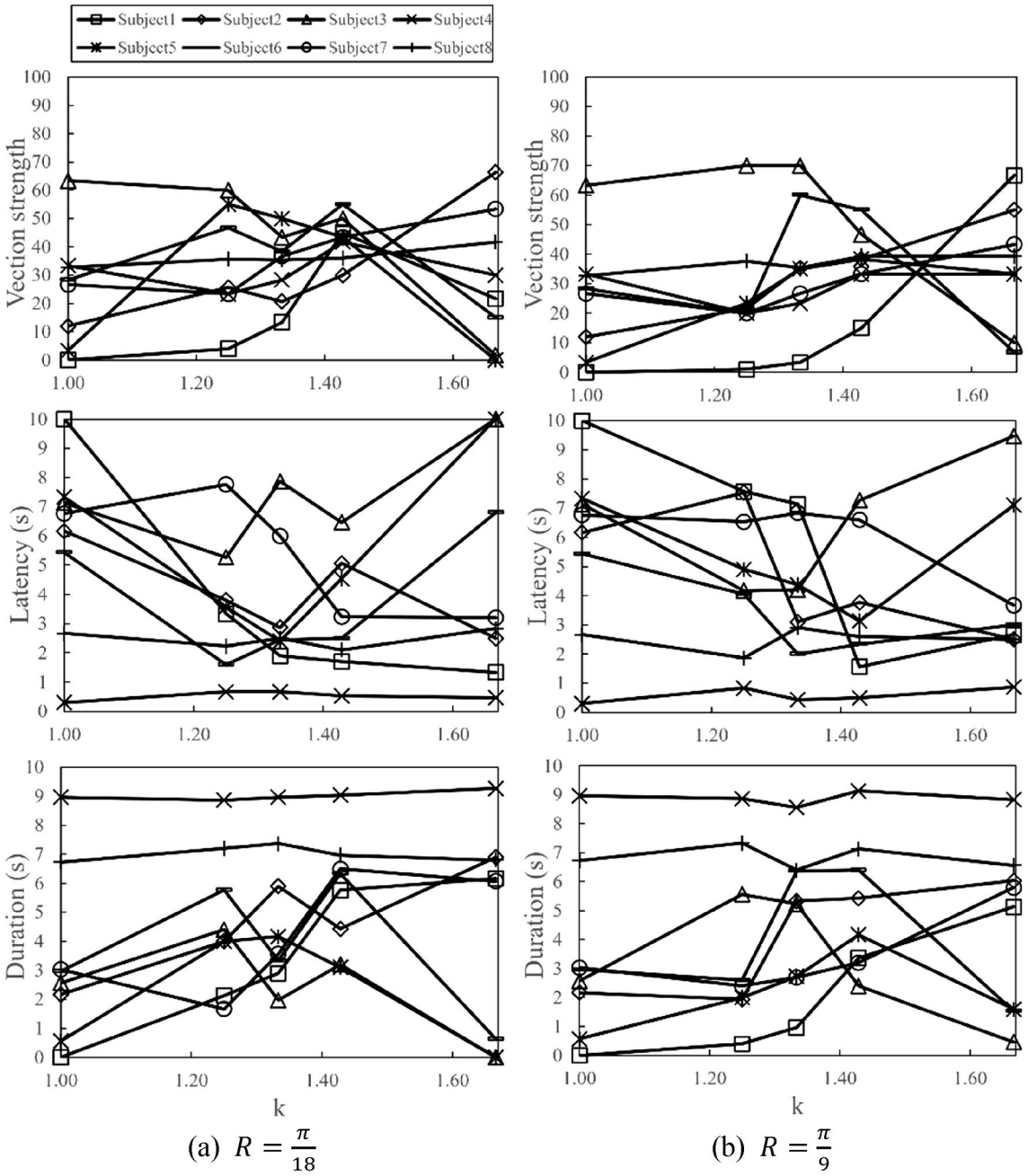

Fig. 7 Result of Experiment 1 (viewing video stretched in right–left direction); **a** R = π/18, **b** R = π/9. The vection strength tends to increase for the stretched video compared to the no-processing video, and vection increases stably and strongly at k = 1.43 and R = π/18

vection strength at $\alpha = 0.1$ and, for $\tau = \frac{\pi}{12}$ or $\frac{\pi}{9}$ in Fig. 9(b) and (c), the vection strength is also best at $\alpha = 0.1$.

As shown in Fig. 9(a), (b), and (c), except for Subject 8, duration and vection strength decreases for adding coefficient $\alpha = 0.2$ for un-processing range $\tau = \frac{\pi}{12}$ and $\tau = \frac{\pi}{9}$. According to the introspective reports of all subjects, expanding grating did not blend naturally with the background live-action video, increasing unnaturalness. Therefore, we consider that excessive processing to the periphery of the visual field does not increase vection strength or duration.

As shown in Fig. 9(a), vection strength and duration increase for un-processing range $\tau = \frac{\pi}{18}$ and adding coefficient $\alpha = 0.2$ as compared to $\alpha = 0$ at the same viewing angle for most of the subjects.

The graphs in Fig. 9(a), (b), (c) show no consistent trend in latency among subjects.

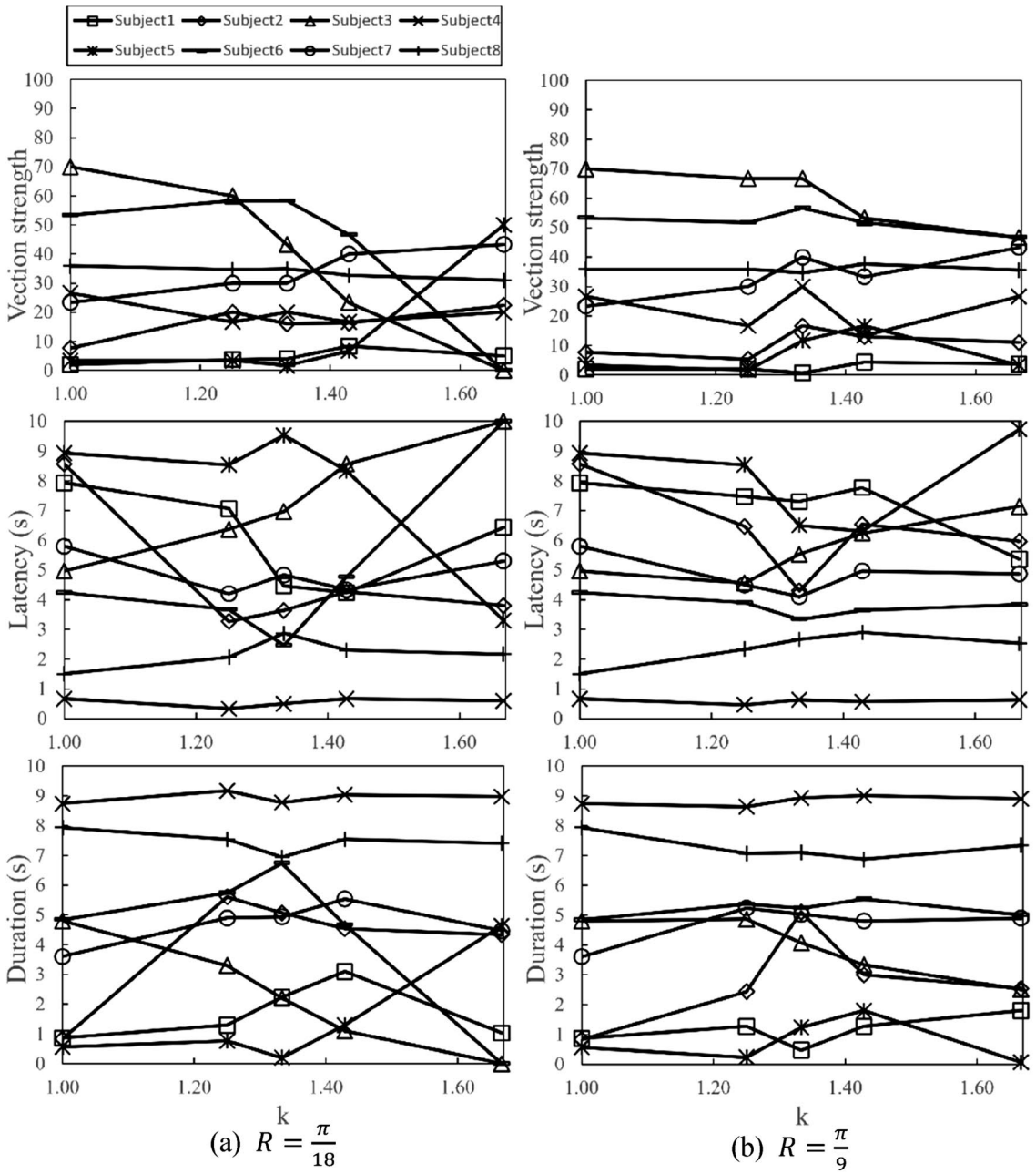

Fig. 8 Result of Experiment 1 (viewing video stretched in downward direction); **a** R = π/18, **b** R = π/9. The vection strength is almost the same regardless of the magnification factor

According to the experimental results, adding coefficient α for the highest vection strength was different for different subjects, but it is the same for the same subject in any un-processing range τ. We assume this is because the best adding coefficient α exists for each subject to perceive the highest vection strength without discomfort. In the future, we will conduct more experiments to clarify whether this assumption is correct.

5 Conclusion

In this paper, we proposed two methods of image processing to increase vection strength. The first applies stretched images in the periphery of the visual field of a live-action video and the second employs an alpha-blended expanding grating.

In Experiment 1, we measured the vection strength, latency, and duration of the first method. The experimental results showed that the vection strength increased with

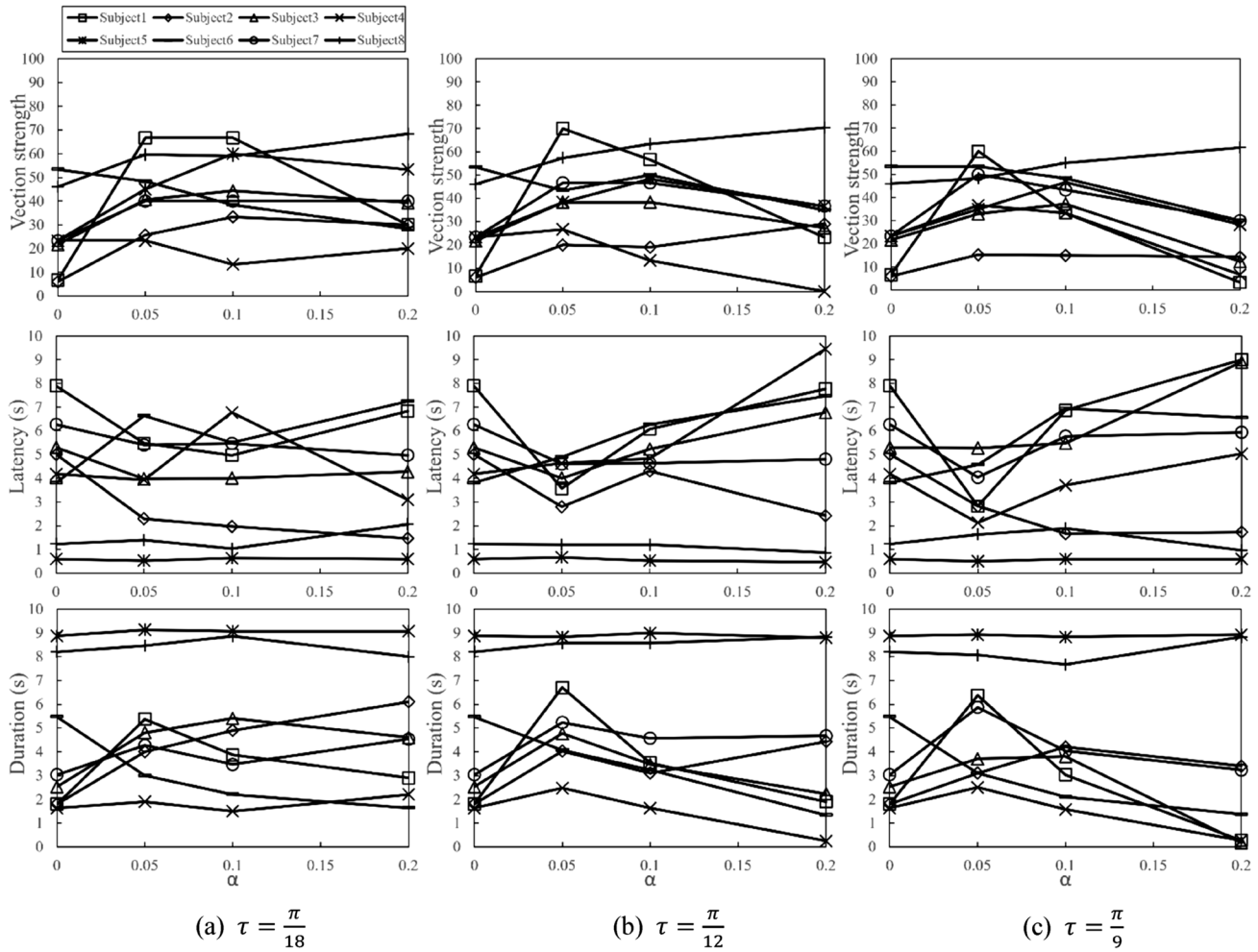

Fig. 9 Results of Experiment 2 (viewing video added expanding grating): **a** $\tau = \pi/18$, **b** $\tau = \pi/12$, **c** $\tau = \pi/9$. Vection strength and duration increased or became nearly flat for adding coefficient $\alpha = 0.05$ and 0.1 compared to $\alpha = 0$ for all un-processing range τ

stretching in the left–right direction, especially with magnification factor $k = 1.43$ and un-processing range $R = \frac{\pi}{18}$. However, the vection strength did not increase when stretching in the downward direction. In Experiment 2, we measured the vection strength, latency, and duration of the second method. The experimental results showed that vection strength and duration increased or nearly flattened by adding expanding grating for most of the adding coefficients α, except for the cases where $\alpha = 0.2$ and un-processing range $\tau = \frac{\pi}{9}$. In particular, when $\alpha = 0.05$, vection strength increased or nearly flattened for all subjects compared to when $\alpha = 0$ (no processing). In both Experiments 1 and 2, videos became more unnatural when the trial videos were stretched or added more strongly, and the vection strength was lower than when viewing unprocessed videos.

One issue is that the experimental video used in this study is degraded as compared to the original video.

The degraded part of the image is not in the center of the field of view, which is the most important part of driving, and, although the peripheral part of the field of view is degraded, the surrounding situation can be grasped, so this is not a serious problem when the degraded image is used in a driving simulator. However, to propose the most appropriate method for driving simulators, this problem needs to be solved.

Effective evaluation methods for degraded images include measuring vection strength, latency, and duration, as well as evaluating whether the subject is correctly grasping the surrounding situation during the driving simulation with video processing and how uncomfortable the images are compared to reality.

There are three possible solutions to degraded images. The first is a method that does not process images of people, cars, and other obstacles that require special attention during driving. The third method is to create differences in the

images by emphasizing the saturation of some parts of the images or the edges of objects in the images, and to enhance vection through visual stimuli that create a depth structure with these differences.

We will consider these methods in the future. We will try to better clarify the relationship between image processing in the periphery of the visual field and vection strength, latency, and duration.

Acknowledgements This study was supported by JSPS Grants-in-Aid for Scientific Research JP19H04155, JP20H05702, JP20K21817, JP20K11919, JP22H00535, and JP23H03485, and by Hoso Bunka Foundation.

Declarations

Conflict of interest The authors declare no conflicts of interest associated with this manuscript. The authors have no conflicts of interest directly relevant to the content of this article.

References

1. Sivak, M., et al.: The information that drivers use; is it indeed 90% visual? Perception **25**(9), 1081–1089 (1996). https://doi.org/10.1068/p251081
2. Okano, Y., et al.: Investigation of stimulus presentation method in the visual periphery to enhance speed sensation (in Japan). IPSJ SIG Technical Reports **2008**(11), 145–150 (2008)
3. Kawashima, Y., et al.: A method of changing motorists' sense of speed by applying visually guided self-motion sensation generated by flashing columnar objects installed on the side of the road to traffic engineering (in Japan). ITE **65**(6), 833–840 (2011). https://doi.org/10.3169/itej.65.833
4. Ito, T., et al.: Time-series effect of optical flow around the driver's viewpoint image on speed perception (in Japan). Human Factors **24**(2), 58–64 (2020). https://doi.org/10.11443/jphf.24.2_58
5. Suzuki, R., et al.: Guiding personal mobility with vection (in Japan). IPSJ Interaction **2017**, 122–126 (2017)
6. Konishi, K., et al.: Analysis of linear vection effects produced by peripheral visual stimuli in an immersive video space (in Japan). IEICE **115**(495), 223–228 (2016)
7. Genba, M., et al.: Research on human-vehicle systems using a large 5-plane stereoscopic driving simulator (in Japan). Transactions of Society of Automotive Engineers of Japan **47**(3), 783–788 (2016)
8. https://www.solidray.co.jp/product/omega/
9. https://www.insta360.com/jp/product/insta360-evo/
10. https://www.vive.com/jp/product/vive-pro-full-kit/
11. https://www.viveport.com/vive-video
12. Fujii, Y., Seno, T.: The effect of optical flow motion direction on vection strength. i-Perception **11**(1), 1–13 (2020). https://doi.org/10.1177/2041669519899108
13. Seno, T., et al.: Wearing heavy iron clogs can inhibit vection. Multisensory Research **26**(6), 569–580 (2013). https://doi.org/10.1163/22134808-00002433
14. Seno, T.: The oscillating potential model of visually induced vection. i-Perception **8**(6) 1–24 (2017). https://doi.org/10.1177/2041669517742176
15. Seno, T.: Does immersion propensity correlate with vection strength? : A challenging study on immersion (in Japan). TVRSJ **21**(1), 3–6 (2016)